COBEM 2021 Florianópolis - Brasil
ABCM Associação Brasileira de Engenharia e Ciências Mecânicas
26th ABCM International Congress of Mechanical Engineering
November 22-26, 2021. Florianópolis, SC, Brazil

COB-2021-0572
COMPARATIVE ANALYSIS OF THE AEROTHERMODYNAMIC PROPERTIES OF A GENERIC SCRAMJET DEMONSTRATOR

Luis Francisco Dias Barreto
Gustavo Lins Freire
José Bismark de Medeiros
Universidade Federal do Vale do São Francisco (UNIVASF), Colegiado Acadêmico de Engenharia Mecânica, Campus Juazeiro, Av.Antonio Carlos Magalhães 510, Santo Antonio, CEP 48.902-300, Juazeiro/BA, Brazil
luis_diaas123@hotmail.com.br, gustavo.lins9857@gmail.com, jose.bismark@univasf.edu.br

Ramon Carneiro
Instituto Tecnológico de Aeronáutica (ITA). Programa de Pós-Graduação em Ciências e Tecnologias Espaciais. Praça Marechal Eduardo Gomes, 50. Vila das Acácias. CEP. 12228-900. São José dos Campos/SP. Brazil.
ramon.carneiro@ga.ita.br

Angelo Passaro
Instituto de Estudos Avançados (IEAv). Trevo Coronel Aviador José Alberto Albano do Amarante. n° 1. Putim. CEP. 12.228-001. São José dos Campos/SP. Brazil.
angelopassaro@gmail.com

Paulo Gilberto de Paula Toro
Universidade Federal do Rio Grande do Norte (UFRN). Centro de Tecnologia. Av. Senador Salgado Filho, 3000 - Campus Universitário, Lagoa Nova CEP 59.078-970 – Natal/RN - Brasil
toro11pt@gmail.com

Abstract. *In 2020, undergraduate students from Aerospace Engineering, at the Universidade Federal do Vale do São Francisco (Juazeiro/BA), began to develop research on hypersonic airbreathing propulsion. In the present work, theoretical-analytical methodology based on equations of the oblique shock wave, and the expansion wave (Prandtl-Meyer) coupled to the area ratio, considering ideal gas (calorically perfect gas), without real gas effects, and inviscid flow (no boundary layer formation), were applied to the compression and expansion sections, respectively, of the preliminary design of a scramjet. Also, numerical simulation (CFD) was developed under the same assumptions (without high temperature and viscous effects) applied in the analytical analysis. In both studies, the heat addition in one-dimensional flow, to simulate the burning of hydrogen fuel with atmospheric air in the combustion chamber at supersonic speed, was not considered. The scramjet vehicle was being designed to operate at an altitude of 20 km at a speed of 1710 m/s, corresponding to Mach number 5.79. The scramjet was composed of three compression ramps and one expansion ramp. The comparison of the analytical and numerical results of the thermodynamic properties, along the scramjet vehicle, showed excellent agreement. Therefore, it is intended, in the near future, to implement the simulation of fuel burning in both studies, theoretical-analytical and theoretical-numerical.*

Keywords: *scramjet, hypersonic airbreathing propulsion, analytical analysis, numerical simulation*

1. INTRODUCTION

Currently, access to space is made by rocket-powered vehicles, and research of new advanced propulsion systems, in particular, airbreathing propulsion are been developed for military or scientific purposes, by several research institutions and universities around the world. Due to the demand for high efficient propulsion systems, the research in hypersonic airbreathing propulsion systems based on supersonic combustion (scramjet) technology to be integrated into an aerospace vehicle to fly, in hypersonic velocity, over five times of sound speed, in the Earth's atmosphere, made the scramjet vehicles of great interest in several research centers, including USA, Australia, China, Russia, European countries (Curran, 2001).

Scramjet vehicles are characterized to use the adequate (wedge or conical shapes) frontal geometry to capture the airflow, from the Earth's atmosphere compressing, decelerating, and canalizing the supersonic airflow to the combustion chamber. At the combustion chamber, fuel at sonic speed is injected into the supersonic airflow. Fuel and air are mixed and burned inside the combustion chamber. The combustion products are expanded at the tail section and the combustion products are delivered into the atmosphere at the same pressure at a given flight altitude.

From the beginning of this century, several supersonic combustion demonstrators have been developed by several countries. In 2002, the scramjet named HyShot 2 developed by the University of Queensland (USQ), Australia, demonstrated by the first time the supersonic combustion during descendent flight at about 30 km geometric altitude, with the hypersonic velocity corresponding to Mach number 7.6, burning hydrogen for about 6 seconds (Hass et al., 2005). In 2004, NASA performed two scramjet flights, known as X-43 (Hyper-X). One demonstrated the supersonic combustion, at the beginning of 2004 at about 30 km of altitude, burning hydrogen for 10 seconds when the X-43 was flying in hypersonic velocity corresponding to Mach number 7 (Marshall et al., 2005a). In November 2004, the X-43, at about the same altitude, burned 10 seconds of hydrogen during flight with Mach number 10 (Marshall et al., 2005b). From 2010 to 2013 US Air Force demonstrated the supersonic combustion close to 30 km of altitude in velocity near five times the sound velocity (Mach number 5), by the missile named X-51, burning hydrocarbon during about 140 seconds (Rondeau and Jorris, 2013).

Currently, the Hexafly-Int is a generic high-speed platform enabling in-flight testing of several breakthrougs technologies, and it is the first International Cooperation on Civil High-Speed Air Transport Research, coordinated by ESA-ESTEC, supported by the EU within the 7th Framework Programme Theme 7 Transport, with the auspices of the European Community (EC) together with 11 partners from Europe (ESA, AIRBUS, CIRA, DLR, ONERA, TET, TSD, GDL, Marotta, University of Stuttgart, VKI), 4 from the Russian Federation (TsAGI, CIAM, LII and MIPT) and 3 from Australia (The University of Sydney, University of New South Wales, USQ) (Steelant et al., 2018).

Also, the Hypersonic International Flight Research Experimentation (HIFiRE) is a program created by the Air Force Research Laboratory (AFRL), developed together with the Australian Defense Science and Technology Organization (DSTO), aims to understand the hypersonics and develop and validate technologies needed to advance in the field of aerospace hypersonic systems (Bowcutt et al., 2012).

Finally, the Instituto de Estudos Avançados (IEAv) is developed a supersonic combustion demonstrator named 14-X, which fulfills the mission of the National Program for Space Activities, and promotes the increase in the participation of the National Industry and the implementation of a program in the mastery of critical technologies, indispensable for the industrial advance and the conquest of the necessary Brazilian autonomy in the strategic space activity (Ricco et al., 2011).

In this work, a preliminary design of a supersonic combustion demonstrator was developed for operation at an altitude of 20km and a hypersonic speed of 1710 m/s (corresponding to Mach number 5.79), considering power-off mode (no hydrogen-air combustion), using theoretical-analytical (engineering approach) and numerical (CFD) methodologies to determine thermodynamic properties and velocities (Mach numbers) from the leading-to-trailing edges. Finally, a comparison of analytical and numerical results was made.

2. METHODOLOGY

The scramjet can be divided into three stations (Fig. 1), namely, according to the methodology presented by Heiser and Pratt (1994) as compression, combustion chamber and expansion sections. The compression section, where the oblique shock wave relationships should be applied, can be divided into two regions: stations 0 to 1, corresponding to external (all incident shock waves converge to the cowl leading-edge) and stations 1 to 3, corresponding internal (only one reflected shock wave, was established at the cowl leading-edge and converges to the combustion chamber entrance). The compression section, stations 0 to 3, provides the airflow in supersonic speed at higher temperature than the fuel ignition temperature. The constant area, from the combustion chamber entrance to fuel injection, namely isolator, at the combustion chamber is used to uniform the flow from the compression section. Fuel at low temperature in sonic speed is injected into supersonic airflow, and burns spontaneously. In general, in the analytical studies the one dimensional (Rayleigh) flow with heat addition theory can be applied to the fuel-air combustion, but it not consider fuel mass addition. In the expansion section, stations 4 to 10, the combustion products are expanding to the Earth's atmosphere, with higher combustion product velocity than the flight scramjet condition, generating installed thrust. Normally, Prandtl-Meyer expansion wave theory coupled to the area ratio theories are applied to the expansion section (Heiser and Pratt, 1994).

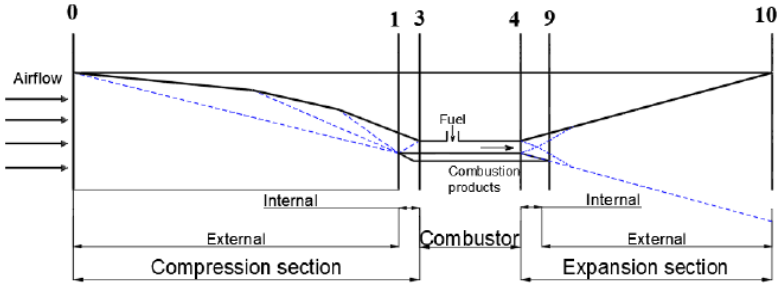

Figure 1. Terminology applied to scramjet vehicles, adapted from Heiser and Pratt (1994).

Basically, ideal gas (calorically perfect gas), no high temperature effects, like dissociation were considered, and no viscous effects (no boundary layer formation) are the hypothesis used to simplify the (mass, momentum and energy) conservation laws and to obtain the oblique shock, one-dimensional (Rayleigh) flow with heat addition, Prandtl-Meyer expansion wave and area ratio theories, which are applied to design the supersonic combustion demonstrator (Anderson, 2003).

The commercial "Fluent" software, which solves the Navier-Stokes (mass, momentum and energy conservation) equations, considering reacting flow and includes routines (solvers) that accurately simulate the behavior of flow, single phase and multiphase, Newtonian and non-Newtonian flow from subsonic to hypersonic speed, is able to perform a numerical theoretical (Computational Fluid Dynamics, CFD) simulation (ANSYS, 2020) applied to any design of the airbreathing propulsion systems based on supersonic combustion to be integrated to an aerospace vehicle to fly into Earth's atmosphere in hypersonic velocities, higher than five times the sound speeds (Mach number higher than 5).

Naidu and Bajaj (2015) and Ramesha et al. (2013) numerically investigated the supersonic airflow inside the nozzle scramjet using the ANSYS Fluent, to validate Fluent's ability to predict reflecting waves and their effect on wall pressure distribution and heat transfer.

Martos et al. (2017) experimental and numerically investigated the airframe-integrated scramjet. The experimental investigation was made in the pulsed hypersonic wind tunnel. Static pressure measurements along with high-speed schlieren photographs were utilized to investigate the hypersonic airflow field along the scramjet model. Pressure measurements along the model were done and compared with the values calculated analytically via shock wave theory and computationally via CFD. Despite the quantitative differences, in general, the experimental and theoretical values exhibit qualitatively the same behavior, but the CFD simulations approximate better to the experimental data. High-speed schlieren photographs compared with the CFD simulations showed that the architecture of the shock waves generated over the scramjet model was consistent with that expected for the shock-on-lip condition at flight Mach number about 7 (on-design condition). Therefore, those results demonstrated the importance of matching theory, ground experiments, and computational simulations in the design of the hypersonic airbreathing vehicle before flight tests.

2.1 Governing equations for theoretical analysis to design scramjet

In the analytical theoretical analysis, the subscripts *in* and *out* are used to identify the upstream (inlet) and the downstream (outlet) conditions, respectively, of each station (Fig. 1) of the generic scramjet inlet baseline.

Oblique shock wave (compression section, Fig. 1): Applying the two-dimensional steady state, compressible flow, non-viscous effects, no heat conduction, and for calorically and/or thermally ideal gas ($p = \rho RT$, $\gamma = \text{constant}$) the oblique shock relationships can be easily obtained as closed form of the shock wave angle β, Mach number across the oblique shock wave, and the thermodynamic property (pressure, density and temperature) ratios (Anderson, 2003), given by:

$$tg\theta_s = 2\left(\text{cotg}\,\beta\right)\left[\frac{\left(M_{in}\ sen\beta\right)^2 - 1}{M_{in}^2\left(\gamma + \cos 2\beta\right) + 2}\right] \tag{1}$$

$$M_{out} = \left[\frac{1}{sen\left(\beta - \theta_s\right)}\right]\sqrt{\frac{\left(M_{in}\ sen\beta\right)^2 + \frac{2}{(\gamma-1)}}{\frac{2\gamma}{(\gamma-1)}\left(M_{in}\ sen\beta\right)^2 - 1}} \tag{2}$$

$$\frac{p_{out}}{p_{in}} = 1 + \frac{2\gamma}{(\gamma+1)}\left[\left(M_{in}\ sen\beta\right)^2 - 1\right] \tag{3}$$

$$\frac{\rho_{out}}{\rho_{in}} = \frac{(\gamma+1)\left(M_{in}\ sen\beta\right)^2}{\left[(\gamma-1)\left(M_{in}\ sen\beta\right)^2 + 2\right]} \tag{4}$$

$$\frac{T_{out}}{T_{in}} = \frac{\frac{p_{out}}{p_{in}}}{\frac{\rho_{out}}{\rho_{in}}} \tag{5}$$

where: ρ, p, T are density, pressure, and temperature of the gas, respectively, function of the incoming local supersonic/hypersonic flow Mach number M_{in}, the gas from the atmosphere γ (air in the Earth's planet, $\gamma = 1.4$) and the oblique shock wave β. For a given deflection (turning) angle θ_s the oblique shock wave β may be obtained iteratively with the relationship $\theta - \beta - M$. Note, the flow across the oblique shock wave promote an increase of pressure, density, temperature, and a decrease of Mach number, however the flow remains supersonic/hypersonic and parallel to the flat surface of the external compression section (Fig. 1).

Prandtl-Meyer and area ratio (expansion section, Fig. 1): At the end of the combustion chamber, the streamlines find a deflection angle, according to the Prandtl-Meyer theory (Eq. 2) establishing a head of the expansion wave (Fig. 1). If the upper and lower surfaces of the expansion section have the same deflection angles, two heads of the expansion waves are established, which intersect equidistantly and establish two reflected heads of the expansion waves. These reflected waves reach the expansion surfaces and define a region where Prandtl-Meyer may be used (Fig. 1) (Anderson, 2003). After the two reflected heads of the expansion waves, the area ratio theory (Eq. 3) should be used (Heiser and Pratt, 1994). Once Mach number after expansion wave M_{out} the thermodynamic property (static pressure, static density and static temperature) ratios may be determined by the closed form given by the isentropic relationships (Anderson, 2003).

$$\mu_{head} = \operatorname{arcsen}\left(\frac{1}{M_{in}}\right) \tag{6}$$

$$\mu_{tail} = \operatorname{arcsen}\left(\frac{1}{M_{out}}\right) \tag{7}$$

$$\theta = \upsilon(M_{out}) - \upsilon(M_{in}) \tag{8}$$

$$\upsilon(M) = \sqrt{\frac{\gamma+1}{\gamma-1}}\ tg^{-1}\sqrt{\frac{\gamma-1}{\gamma+1}\left[M^2-1\right]} - tg^{-1}\sqrt{M^2-1} \tag{9}$$

$$\frac{T_{out}}{T_{in}} = \left(\frac{1+\frac{\gamma-1}{2}M_{in}^2}{1+\frac{\gamma-1}{2}M_{out}^2}\right) \tag{10}$$

$$\frac{p_{out}}{p_{in}} = \left(\frac{T_{out}}{T_{in}}\right)^{\frac{\gamma}{\gamma-1}} \tag{11}$$

$$\frac{\rho_{out}}{\rho_{in}} = \frac{\frac{p_{out}}{p_{in}}}{\frac{T_{out}}{T_{in}}} \tag{12}$$

where: μ_{head} and μ_{tail} are the head and tail of the expansion wave angles, respectively. θ is the deflection (turning) expansion wave angle. υ (M) is the Prandtl-Meyer function.

$$\frac{A_{out}}{A_{in}} = \frac{M_{in}}{M_{out}} \left(\frac{1 + \frac{\gamma - 1}{2} M_{out}^2}{1 + \frac{\gamma - 1}{2} M_{in}^2} \right)^{\frac{\gamma+1}{2(\gamma-1)}} \tag{13}$$

Note the flow across the expansion wave (Prandtl-Meyer and area ratio) promote a decrease of static pressure, static density, static temperature, and an increase of Mach number. The flow remains supersonic/hypersonic and parallel to the flat surface of the internal and external expansion section (Fig. 1) of the hypersonic vehicle with airframe-integrated scramjet engine lower surface.

2.2 Numerical theoretical simulation

The numerical theoretical simulation (CFD) of the supersonic combustion demonstrator can be solved by the government equations (in two dimensions) known as Navier-Stokes equations. Considering inviscid flow, the Navier-Stokes equations became the Euler equations (inviscid case), which represent the principles of nature (conservation of mass, conservation of momentum and conservation of energy). The ANSYS Fluent solves simultaneously all the integral governing equations (continuity, momentum, and energy) simultaneously and provides the density-based solver, to obtain the velocity and density fields.

3. RESULTS AND COMMENTARIES

The UNIVASF scramjet was generated from a computational routine developed based on the criteria described by Carneiro (2020), considering the use of three ramps at the compression section (Fig. 2), the maximum height of 380mm, and the use of hydrogen as fuel. The calculated geometry has a leading-edge angle of 7.25º, followed by two deflection angles of 8.6º and 10.3º, flying at 20 km of geometric altitude with speed 1710 m/s corresponding at Mach number 5.79 were analytically and numerically investigated.

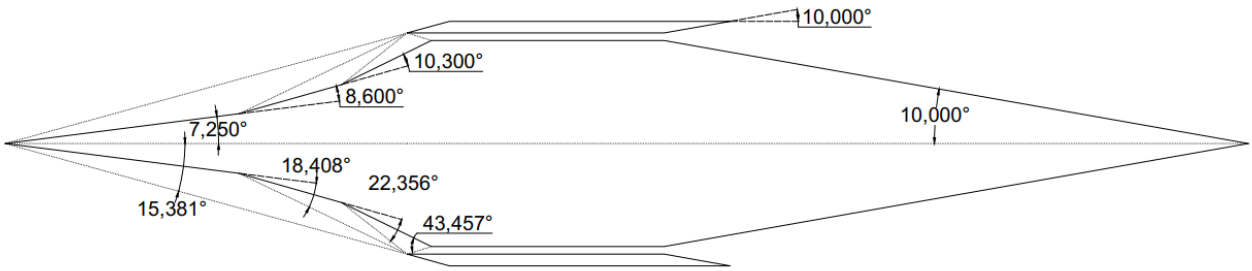

Figure 2. UNIVASF scramjet geometry for analytical and numerically studied.

The thermodynamic atmospheric air properties (Tab. 1) were obtained from the U.S. Standard Atmosphere (1976). The scramjet compression section with three compression ramps (Fig. 2), considering shock on-lip (all incident shock converged to the cowl leading-edge) and shock on-corner (the only reflected shock converged to combustion chamber entrance) conditions, satisfy the combustion chamber entrance conditions of temperature T_3 and supersonic velocity, corresponding to Mach number M_3, to spontaneously burns the hydrogen-air mixture, at fuel (hydrogen) ignition temperature of 845 K.

Table 1. Thermodynamic properties of the atmospheric air at 20 km altitude.

Thermodynamic properties of the atmospheric air (U.S. Standard Atmosphere, 1976)					Flight conditions	
Altitude	Temperature	Pressure	Density	Sound speed	Velocity	Mach number
km	K	Pa	kg/m^3	m/s	m/s	-
20	216.65	5529.02	0.0889	295.06	1710	5.79

3.1 Analytical (engineering approach) analysis

The thermodynamic properties and the supersonic velocities (and corresponding Mach numbers), of the airflow from the leading-to-trailing edges, were obtained by applying the oblique shock wave and Prandtl-Meyer expansion wave coupled to the area ratio theories. With this objective, calculations described in section 2.1 are solved from a computational routine developed based on the following criteria: air as ideal gas (calorically perfect gas) and no viscous effects, the results were shown at Tab. 2. For the constant area combustion chamber, no hydrogen-air combustion, the thermodynamic properties and velocity (Mach number) at the combustion chamber outlet were the same as the combustion chamber inlet (Tab. 2). The expansion wave (Prandtl-Meyer) relationships were used up to the head of the reflected expansion wave hits the expansion section of the scramjet. After that, the area ratio equations should be applied to the trailing edge of the expansion section (Tab. 2). The reflected head of the expansion wave was assumed to be the same, and equal to the incident head of the expansion wave.

The oblique shockwave provided an increase of pressure, temperature, density, and speed of sound; and a decreased of flow velocity (Mach number), and the streamline of the airflow remained supersonic and parallel to the surface (Tab. 2) of the generic scramjet compression section. Also, pressure ratio, temperature ratio, density ratio as well as the product Min sin β are constant for all incident shock waves, characteristics of the same shock strength (Ran e Mavris, 2005). Also, the flow across the expansion wave and area ratio, the thermodynamic properties decreased and flow velocity (Mach number) increased. Finally, the total temperature from the leading-to-trailing edges was constant, since there was no heat addition, means, no hydrogen-air combustion. Therefore, the airflow velocity was slight lower than the flight scramjet condition, 20 km, 1710 m/s, and Mach number 5.79 (Tab. 2).

Table 2. Thermodynamic properties at the generic scramjet, altitude 20 km, flight velocity 1710 m/s. Power-off.

		Flight conditions	Compression section				Combustion chamber section		Expansion section	
									Prandtl-Meyer	Area ratio
		Station 0	1ª ramp	2ª ramp	3ª ramp	Reflection	Inlet	Outlet	Station 4	Station 9
M_{in}	-	5.79	5.79	4.87	4.04	3.29	1.81	1.81	1.81	2.17
θ	º		7.25	8.6	10.3	26.15			10	10
β	º		15.38	18.41	22.36	43.47				
M_{in}senβ	-		1.54	1.54	1.54	2.27				
M_{out}	-		4.87	4.04	3.29	1.81	1.81	1.81	2.17	5.32
p_{out}/p_{in}	-		2.59	2.59	2.59	5.83	1	1	0.57	0.01
T_{out}/T_{in}	-		1.34	1.34	1.34	1.92	1	1	0.85	0.29
ρ_{out}/ρ_{in}	-		1.92	1.92	1.92	3.04	1	1	0.67	0.05
p	Pa	5529.02	14319.39	37075.54	96024.47	559487.83	559487.83	559487.83	318787.54	4294.80
T	K	216.65	291.41	391.93	527.19	1010.25	1010.25	1010.25	860.26	251.80
ρ	kg/m^3	0.0889	0.1712	0.3296	0.6345	1.9294	1.9294	1.9294	1.2910	0.0595
a	m/s	295.06	342.21	396.87	460.28	637.16	637.16	637.16	587.97	317.78
u	m/s	1710	1665.49	1603.71	1516.62	1153.05	1153.05	1153.05	1277.06	1689.52
T	K	1671.93	1671.93	1671.93	1671.93	1671.93	1671.93	1671.93	1671.93	1671.93

3.2 Numerical (CFD) analysis

For the numerical analysis, the academic version of the ANSYS Fluent software was used. The same hypotheses of the analytical analysis were considered for the airflow, a calorically perfect gas and no viscous effects. In order to compare with the analytical results, the numerical investigation was modeled as power-off configuration (no hydrogen-air combustion). In the construction of the domain, the longitudinal symmetry of the scramjet was used to reduce the computational effort, the other boundaries of the domain were defined as Pressure Far-Field for the input region, a condition that requires the setting of the velocity of the thermodynamic properties of atmospheric air at 20 km of altitude, and finally the Pressure outlet condition that comprises the output region of and domain flow (Fig. 3a). Two-dimensional, steady state, non-viscous, no heat conduction compressible flow using implicit second order upwind spatial discretization were used to nose-to-tail numerical modeling of the scramjet vehicle, in this work.

A mesh of quadrilateral elements, of the type structured with 509500 numerical cells and 511460 grid nodes (Fig. 3b) were used to the nose-to-tail numerical modeling of the scramjet (Fig. 2), the input properties were defined in the pressure far-field region, as defined in Table 1. A high grid resolution was applied to the region where the presence of the oblique shock and expansion waves were expected, according to the 2-D non-viscous calorically perfect hypersonic airflow analytical theoretical analysis.

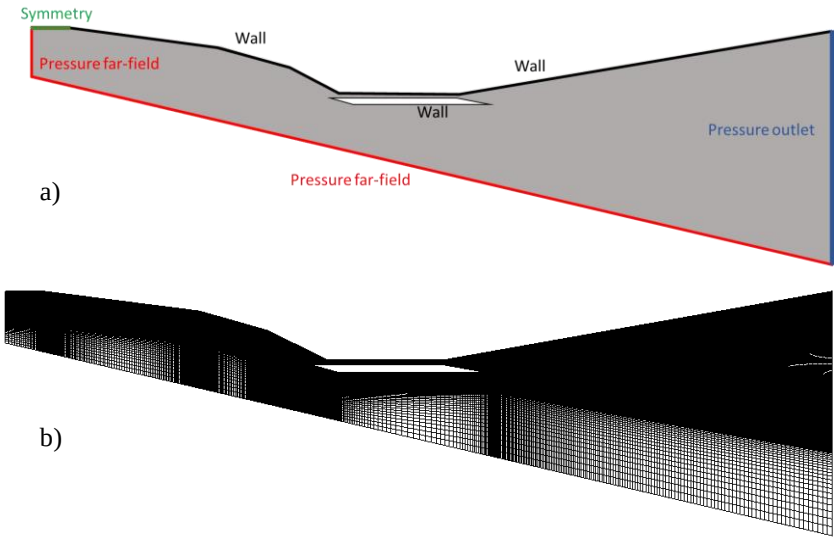

Figure 3. Computational mesh and domain of the scramjet numerical model.

The Mach number contour (Fig. 4) showed that there was no shock train at the combustion chamber inlet, due to the both incident oblique and the reflected shock waves. Therefore, shock on-lip and shock on-corner conditions were satisfied (Fig. 5). One can observe the velocity (and corresponding Mach number) decreased in the external and internal compression section, remained constant due to no hydrogen-air combustion, and increased in the expansion section (Figs. 6 and 4).

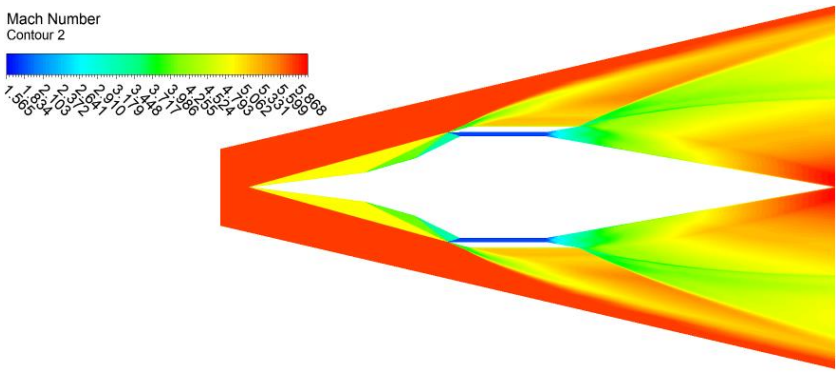

Figure 4. Mach number contour.

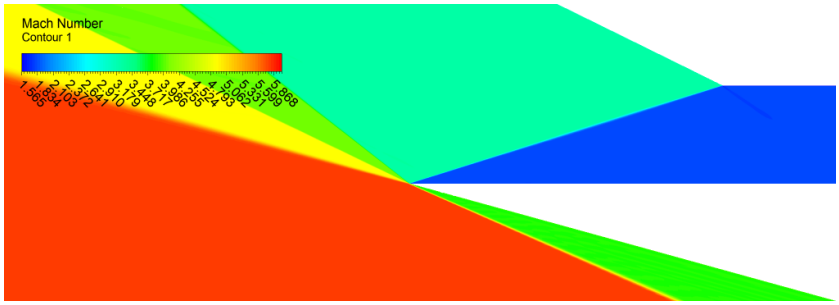

Figure 5. Mach number contour at the entrance of the combustion chamber.

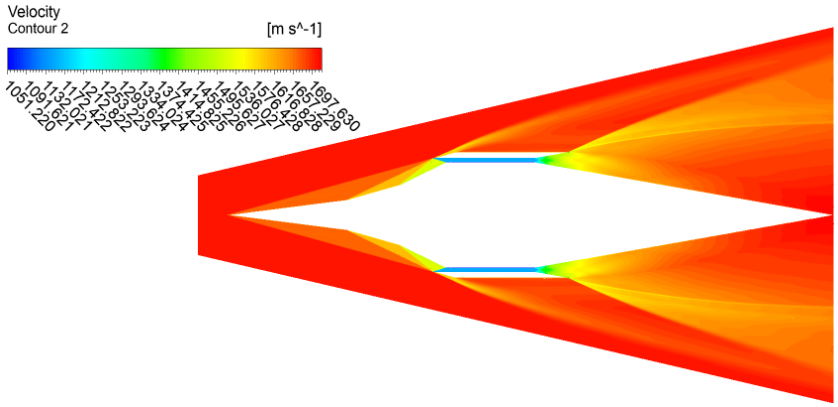

Figure 6. Airflow velocities from leading-to-trailing edges.

For the present numerical test case, with power-off (no hydrogen-air combustion), the air flow from the (external and internal) compression section were deflected to the combustion chamber inlet, and the combustion chamber inlet airflow properties (pressure, temperature, density) and the supersonic velocity (Mach number) remaining constant up to the exit of the combustion chamber.

The 7.25° leading-edge deflection angle following by ramps with 8.6° and 10.3° were capable to generate a static temperature about 1010 K (Tab. 2) at the combustion chamber (Fig. 7) higher than the hydrogen ignition temperature of 845 K (Kuchta, 1985), with supersonic air velocity of 1153 m/s (Fig. 6) and Mach number of 1.81 (Tab. 2) at the combustion chamber (Fig. 4).

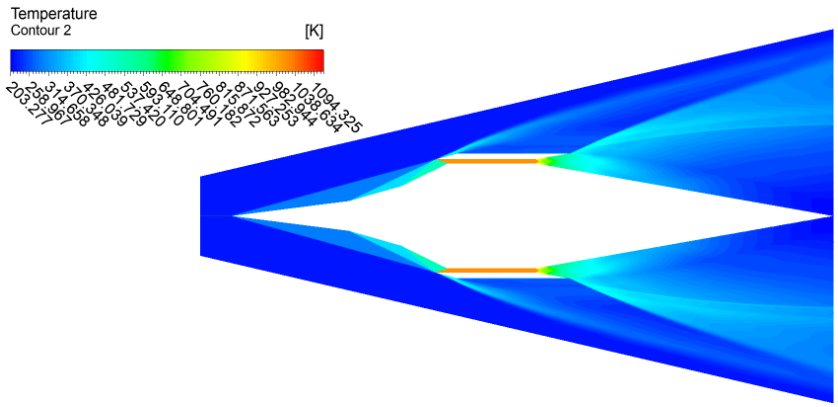

Figure 7. Temperature contour.

The maximum static pressure (Tab. 2) occurred at the combustion chamber (Fig. 8) and may be used as a guide to specify the fuel injection layout and conditions to the static and dynamic structural analysis. Schlieren pictures, which are based on density gradients, taken from the experimental investigations may be compared with the density contour (Fig. 9). Note that, the interaction of the hypersonic Mach number 5.79 with the 7.25° attached leading-edge deflection angle established a weak density gradient in comparison with the 8.6° compression ramp.

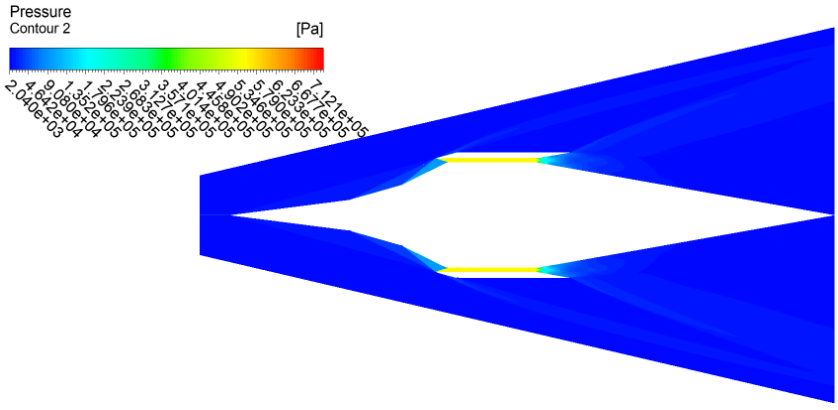

Figure 8. Pressure contour.

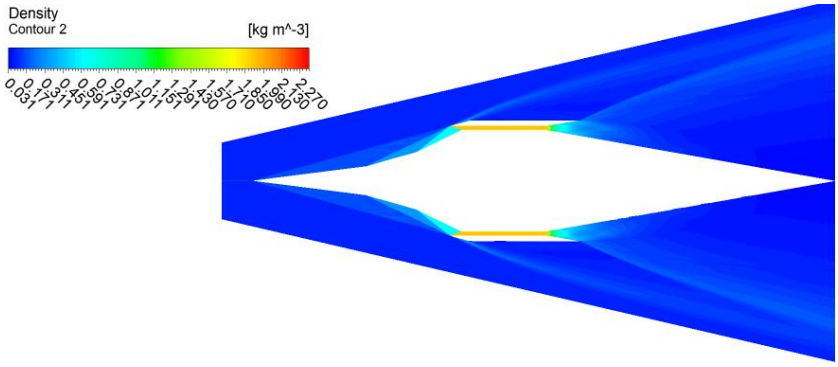

Figure 9. Density contour.

3.3 Comparision of analytical (engineering approach) and numerical analysis

Analytical (engineering approach) and numerical methodologies were used to determine the thermodynamic airflow properties, pressure (Fig. 10), temperature (Fig. 11), and the airflow velocity (Fig. 12) and Mach number (Fig. 13).

Observe in the compression section the values of the thermodynamic properties increased while the airflow velocity (Mach number) decreased. On the other hand, in the expansion section occurred the opposite, the thermodynamic properties decreased and the airflow velocity (Mach number) increased. Since there was no hydrogen burning, the exit airflow conditions were the same as the conditions at the combustion chamber entrance.

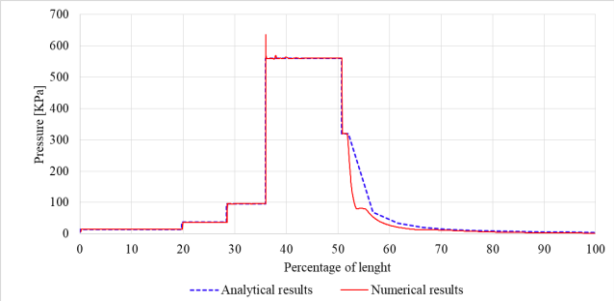

Figure 10. Pressure distribution.

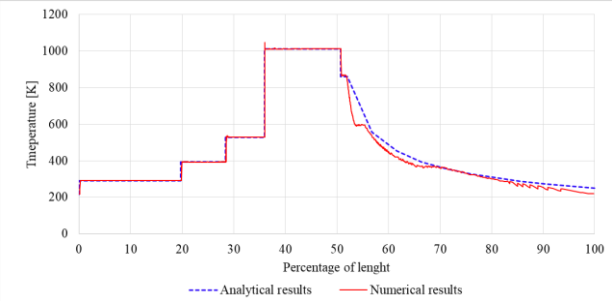

Figure 11. Temperature distribution.

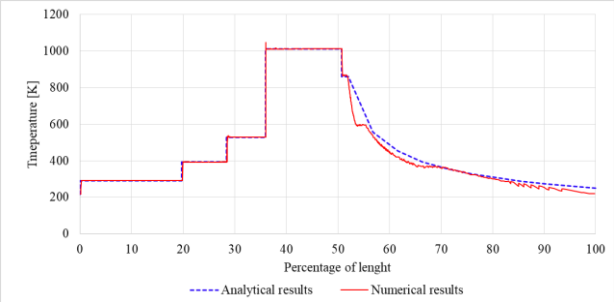

Figure 12. Velocity distribution.

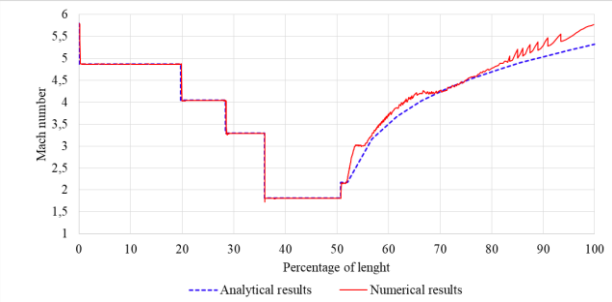

Figure 13. Mach number distribution.

4. CONCLUSIONS

A 2-D generic scramjet design is being developed at the Universidade Federal do Vale do São Francisco (UNIVASF), to demonstrate in atmospheric flight the supersonic combustion, of atmospheric air (in supersonic speed) with hydrogen, in flight conditions: 20 km, 1710 m/s, corresponding to Mach number 5.79.

The thermodynamic properties and airflow velocity (corresponding to Mach number) from leading-to-trailing edges (compression, combustion chamber and expansion sections) of the generic scramjet were estimated applying the oblique shock wave and the Prandtl-Meyer expansion wave coupled to the area ratio theories, considering ideal gas assumptions (no high-temperature effects, no dissociation or ionization) and no viscous effects (no boundary layer formation).

In the present work, the analytical (engineering approach) theoretical analysis and the numerical theoretical simulations, which quantify the continuity equations of mass, momentum and energy (Euler's equations) for inviscid airflow, were used, and both results agreed very well.

Firstly, the generic scramjet, with three ramps at the compression section (with leading-edge angle of 7.25º, followed by two deflection angles of 8.6º and 10.3º), flying at 20 km of geometric altitude with velocity of 1710 m/s (corresponding at Mach number 5.79) was capable to generate a supersonic velocity of 1153 m/s (corresponding to Mach number of 1.81) and a static temperature of 1010 K, higher than 845 K (hydrogen ignition temperature) at the entrance of the combustion chamber.

The capability of an in-house code as an aerothermodynamic tool for the preliminary supersonic combustion demonstrator design of scramjet engines had been assessed. Further, the good agreement about analytical and numerical investigations presented in this work was the first step to acquire the knowledge needed to make the in-house code, applying the engineering approach, including one-dimensional (Rayleigh) flow with heat addition, to simulate the hydrogen-air combustion.

As future work, not only boundary layer (viscous effects) and high-temperature effects, but also the one-dimensional (Rayleigh) flow with heat addition (to analyze the hydrogen-air combustion) and the scramjet thrust, should be considered for the generic scramjet design.

5. ACKNOWLEDGEMENTS

This study was financed in part by the Coordenação de Aperfeiçoamento de Pessoal de Nível Superior - Brasil (CAPES) - Finance Code 001. This work was carried out with the support of the Academic Cooperation Program in National Defense (PROCAD-DEFENSE), grant 88881.387753/2019-01. The authors would like to thank the Universidade Federal do Vale do São Francisco (UNIVASF). The three last authors to extend their gratitude to the Instituto Tecnológico de Aeronáutica (ITA) to support granted to carry out research on hypersonic airbreathing propulsion. The fifth author extends his gratitude to Instituto de Estudos Avançados (IEAv). Finally, the last author would like to thanks the Universidade Federal do Rio Grande do Norte (UFRN)

6. REFERENCES

Anderson Jr., J. D. (2003) Modern Compressible Flow: with Historical Perspective. McGraw-Hill series in Aeronautical and Aerospace Enginnering. Third Edition. ISBN O-07-242443-5. ISBN 0-07-1 12161-7 (ISE).

BOWCUTT, K.; PAULL, A.; DOLVIN, D.; SMART, M. HIFiRE: an international collaboration to advance the science and technology of hypersonic flight. 28th International Congress of the Aeronautical Sciences (ICAS). Brisbane/Australia. 2012.

Carneiro, R. Analytical Study of the Supersonic Combustion Technology Demonstrator. 2020. 120 p. Master's Dissertation (Graduate Program in Mechanical Engineering) – Universidade Federal do Rio Grande do Norte, Natal-RN, 2020.

Curran, E. T. (2001) Scramjet Engines: The First Forty Years. (AIAA) Journal of Propulsion and Power, 17(6), 1138–1148. doi:10.2514/2.5875

Hass, N., Smart, M., & Paull, A. (2005). Flight Data Analysis of the HyShot 2. AIAA/CIRA 13th International Space Planes and Hypersonics Systems and Technologies Conference. doi:10.2514/6.2005-3354

Heiser, W.; Pratt, D.; Daley, D.; Mehta, U. (1994) Hypersonic Airbreathing Propulsion. AIAA Education Series. ISBN 1-56347-035-7. https://doi.org/10.2514/4.470356

Kuchta, J. M., Investigation of Fire and Explosion Accidents in the Chemical, Mining, and Fuel-Related Industries – a Manual, Bulletin 680, U.S. Bureau of Mines, 1985, Appendix A.

Marshall, L. A.; Bahm, C.; Corpening, G. P.; Sherrill, R. Overview with results and lessons learned of the X-43A Mach 10 flight. AIAA/CIRA 13th International Space Planes and Hypersonic Systems and Technologies Conference. Capua/Italy. (AIAA 2005-3336). 2005.

Marshall, L. A.; Corpening, G. P.; Sherrill, R. A. Chief engineer's view of the NASA X-43A scramjet flight test. AIAA/CIRA 13th International Space Planes and Hypersonic Systems and Technologies Conference. Capua/Italy. (AIAA 2005-3332). 2005.

Martos, J. F. A., Rêgo, I. S., Pachon Laiton, S. N., Lima, B. C., Costa, F. J., and Toro, P. G. P. (2017). Experimental Investigation of Brazilian 14-X B Hypersonic Scramjet Aerospace Vehicle. International Journal of Aerospace Engineering, 2017, 1–10. doi:10.1155/2017/5496527

Naidu K.S. and Bajaj D.K. (2015). Modelling and Exhaust Nozzle Flow Simulations in a Scramjet. Journal of Astrophysics and Aerospace Technology, 03(02). doi:10.4172/2329-6542.1000122

Ramesha D.K., Rudra M., Hemanth Kumar, P. (2013) CFD Analysis of Supersonic Exhaust in a Scramjet Engine. International Journal of Innovative Research in Science, Engineering and Technology. Vol. 2, Issue 9, September 2013.

Ran, H., and Mavris, D., Preliminary Design of a 2D Supersonic Inlet to Maximize Total Pressure Recovery, 2005.

Ricco, M.F.F., Funari, P.P., Carvalho, A.V., 2011, Espaço, Tecnologia, Ambiente e Sociedade (in Portuguese), 1st Ed., Habilis Editora Erechim, RS, Brazil, Chapter 8, 161.

Rondeau, C. M.; Jorris, T. R. X-51a scramjet demonstrator program: waverider ground and flight test. SFTE 44th International / SETP Southwest Flight Test Symposium, Fort Worth, Texas/EUA. 2013.

Steelant, J.; Villace, V.; Kallenbach A.; Wagner, A.; Andro, J.; Benedetto, S.; et al. Flight testing designs in HEXAFLY-INT for high-speed transportation. HISST 2018. Moscou/Russia. (hal- 01978022). 2018.

U.S. Standard Atmosphere. (1976). NASA TM-X 74335. National Oceanic and Atmospheric Administration, National Aeronautics and Space Administration and United States Air Force.

7. RESPONSIBILITY NOTICE

The Authors are the only responsible for the printed material included in this scientific article.
The Authors declare that there is no conflict of interest regarding the publication of this scientific article.